Computational Materials Science 146 (2018) 26–35

Contents lists available at ScienceDirect

Computational Materials Science

journal homepage: www.elsevier.com/locate/commatsci

Influence of SiC surface defects on materials removal in atmospheric pressure plasma polishing

Guanglu Jia [a], Bing Li [a], Jufan Zhang [a,b,*]

[a] School of Mechanical Engineering and Automation, Harbin Institute of Technology Shenzhen, Guangdong 518055, China
[b] Centre of Micro/Nano Manufacturing Technology (MNMT-Dublin), School of Mechanical and Materials Engineering, University College Dublin, D04E4X0, Ireland

ARTICLE INFO

Article history:
Received 7 December 2017
Received in revised form 8 January 2018
Accepted 9 January 2018

Keywords:
Atmospheric pressure plasma polishing
SiC
Chemical etching
Surface defect
Removal rate

ABSTRACT

To study the influence of SiC surface defects on atmospheric pressure plasma polishing (APPP) process, quantum chemistry simulation and analysis is used to reveal the reaction features of typical defect topographies. Three groups of typical structures are modeled, including edge dislocation, screw dislocation and perfect crystal lattice. By using quantum chemistry calculation software, it is demonstrated that the existence of surface defects improves probability for chemical etching. The densities of states (DOS) and number of bonding electrons indicate that the defect structures have poor stability compared with perfect crystal lattice, which means defects are favorable for increasing the removal rate. The calculation results on activation energy also verify the conclusion further. Experimental machining and measurement have been performed to prove the theoretical analysis. Tests are made on selected single crystal SiC samples with different defect densities. Removal profiles measured by white light interferometer indicate that surface defects are helpful for raising the machining efficiency. But, measured surface topographies show that within certain range, surface defects deteriorate the surface roughness during the polishing process. Until most surface damage is removed, the surface roughness will be improved effectively which makes the interface smoother. Thus, the experimental investigation accords well with theoretical analysis.

1. Introduction

Silicon carbide (SiC) has drawn much attention due to its excellent properties and potential applications in various fields [1–5]. But the extremely high hardness of SiC brings a number of challenges to manufacturing technologies [6]. Especially for increasing the machining efficiency, large cutting force is usually applied on SiC surface which causes serious surface/subsurface defects. Crystal defects have a great unfavorable effect on physical and chemical features, such as electrical conductivity, strength of extension, etc [7–10]. For example, Tanimoto et al. gave special focus on the degradation of the switching characteristics due to carrier trapping at SiC/SiO_2 interface defects [11]. Wu et al. discussed some typical surface defects on the laser-ablated surfaces [12]. It is especially noteworthy that the outside instantaneous stress always causes disastrous consequence and leads to component scrap [13]. So some new ways have been developed recent years in order to obtain high-quality surfaces with minimum surface/subsurface damage, such as float polishing, plasma assisted chemical etching, ion beam polishing, magnetorheological polishing and so on [14–17]. Boukezzata et al. investigated the formation of thin porous amorphous silicon carbide (PASiC) by Al assisted photochemical etching [18]. Pitthan et al. removed the silicon dioxide film by HF etching while studying the influence of SiC reacting with CO in SiC metal-oxidesemiconductor (MOS) devices [19]. Zhang et al. reported that the shallow damage layer is usually eliminated effectively by applying Atmospheric Pressure Plasma Polishing (APPP) [20]. APPP is chemical in nature which makes it much favorable for removing former surface damage and achieve high quality surfaces. As the lattice defects indicate different reaction features compared with perfect lattice structures, it is meaningful to discuss the influence of surface defects on materials removal process, especially when the samples are under ultra-precision machining. This paper aims at revealing the general impacting rules of surface defects on removal process of APPP, especially on the removal rate and surface roughness. Quantum chemistry simulation and analysis method is introduced to investigate the interface reaction process, which is really an innovative attempt on mechanism study. Moreover, to overcome the disadvantage that microscopic study at atomic scale is difficult to be testified by actual macroscopic experiments, the simulation and experiments are designed carefully to realize possible comparison. It is significant

* Corresponding author at: School of Mechanical Engineering and Automation, Harbin Institute of Technology Shenzhen, Guangdong 518055, China.
E-mail address: zhangjufan@hit.edu.cn (J. Zhang).

https://doi.org/10.1016/j.commatsci.2018.01.025
0927-0256/

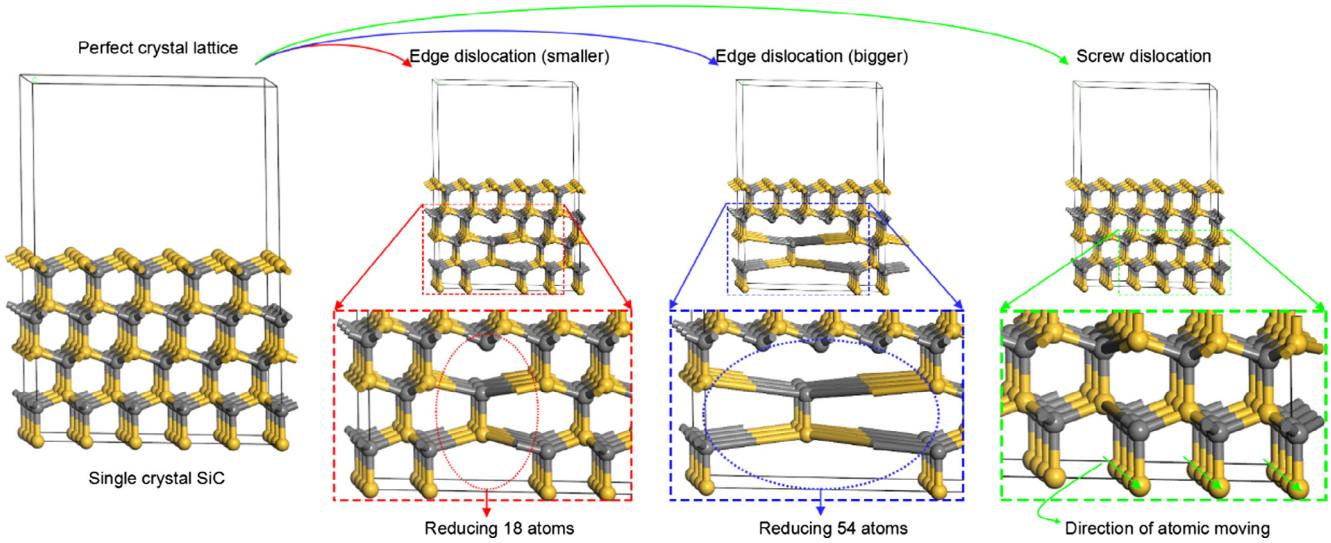

Fig. 1. Four typical models: perfect lattice structure of single crystal SiC, SiC structure with small edge dislocation, large edge dislocation and screw dislocation.

to reveal the unique features of removing damage layer in chemical etching process. The conclusions are very helpful for instructing the optimization of process parameters.

2. Quantum chemistry modeling

CASTEP and DMol^3 program packages within Materials Studio software (4.0, Accelrys Software Inc.) are used for calculation. To qualitatively investigate the reaction difference between defect structures and perfect lattice structure, four typical models are built as Fig. 1 shows, including the perfect SiC structure, the small edge dislocation structure, the large edge dislocation structure and the screw dislocation structure.

Comparisons are intended to be made for different model groups, which is useful to identify the impacting rules of defect style and defect density. Geometrical optimization is made on all the models using Perdew-Wang generalized-gradient approximation (GGA-PW91) [21]. Then band structure, DOS and number of bonding electrons are calculated.

In CASTEP, the cutoff energy is set to be 300.0 eV by extensive tests to guarantee both the calculation speed and accuracy. The total energy tolerance is $2 * 10^{-5}$ eV/atom, and density mixing is chosen as the electronic minimizer with charge 0.3. In addition, although converting to higher symmetry can significantly improve the speed of calculation, P1 symmetry is applied in order to make reaction preview successfully.

For DMol^3, DFT (density functional theory) is applied to simulate chemical reaction rapidly and accurately [22]. The GGA with the Perdew-Burke-Ernzerh (PBE) exchange correlation function is adopted [23], with the DND basis set properly chosen. The transition state search is carried out and verified with vibrational analysis by employing Linear synchronous transit/quadratic synchronous transit (LST/QST) transition state search algorithm. The value of SCF tolerance and maximum SCF cycles are set by 0.001 and 3000, respectively. A thermal smearing value of 0.005 Ha is used. The charge value 0.003 and selected spin density mixing parameters also work well for the convergence of the self-consistent calculations.

3. Results and discussion

3.1. Influence of surface defects on removal rate

The partial density of states (PDOS) and total density of states for the Si and C atoms are presented in Fig. 2 to analyze the composition which determines the band structure. Fig. 2a, c, e presents the DOS for reactants of perfect single crystal SiC model, small edge dislocation model and screw dislocation model, respectively. The DOS for products of three systems are shown in Fig. 2b, d, f, respectively.

It is obvious that the band from −17 eV to −11 eV is originated from the C 2s states. The band between about −11 eV and −7.4 eV is controlled by the C 2p states and Si 3 s states. The band in the range of around −7.4 eV to −1 eV is mainly contributed to the C 2p and Si 3p states. The band around the Fermi level is formed by the Si 3p states as shown in Fig. 2a. In Fig. 2c, it is clear that the band between −16 eV and −10 eV is controlled by the C 2s states. The band from −10 eV to the Fermi level and around Fermi level are originated from C 2p states and Si 3p states, respectively. In Fig. 2e, similar conclusion can be drawn that the lower band (between −17 eV and −11.5 eV) is contributed to the C 2s states, while the middle band (from −10.5 eV to −7.2 eV) is mainly formed by the C 2p states and Si 3s states. Another band (between −7.2 eV and 1.5 eV) are mainly formed by the C 2p states and Si 3s states. The position of DOS for Si-F can be found by comparing reactants and products in each system, which is at around −24.8 eV, −23 eV and −26 eV for the perfect crystal lattice, edge dislocation structure and screw dislocation structure, respectively.

To investigate the different reaction features of three systems, comparison is made on PDOS of free F atoms and Si atoms bonding with F as shown in Fig. 3.

Fig. 3a shows that the bonding between F and the surface is indicated by the overlap of the p-orbital of Si with the s-orbital of F, which is primarily in the range of −26 eV to −25 eV below the Fermi level. Then similar conclusion can be obtained from Fig. 3b and c. However, it should be noted that the overlap of the p-orbital of Si with the s-orbital of F in Fig. 3a is more than others, which means that the strength of bonding between F and Si in the dislocation models is weaker than that of perfect lattice model. So, conclusions can be drawn that the stability of perfect lattice Si-F system is the strongest among these. That is to say, the lattice with dislocation can be etched more easily than the perfect crystal lattice.

The number of states can be calculated by using integrated DOS function, which is shown in Fig. 4.

Fig. 4a presents the number of states for the reactants of each system, while the numbers of states for products are shown in Fig. 4b. In Fig. 4a, it is clear that the numbers of states are 124.35859, 119.7511, 122.43768 around the Fermi level for three